Glial cells generate neurons: the role of the transcription factor Pax6

Nico Heins[1], Paolo Malatesta[1], Francesco Cecconi[2], Masato Nakafuku[3], Kerry Lee Tucker[4], Michael A. Hack[1], Prisca Chapouton[1], Yves-Alain Barde[2] and Magdalena Götz[1]

[1] *Max-Planck Institute of Neurobiology, Am Klopferspitz 18a, 82152, Planegg-Martinsreid, Munich, Germany*

[2] *Dipartimento di Biologia, Universita degli studi 'Tor Vergata', Via della Ricerca Scientifica, 00133 Rome, Italy*

[3] *University of Tokyo, Graduate School of Medicine, 7-3-1 Hongo, Bunkyoku, Tokyo, 113-0033 Japan*

[4] *Friedrich Miescher Institute for Biomedical Research, Maulsbeerstr. 66, 4058 Basel, Switzerland*

P.M. and N.H. contributed equally to this work

Correspondence should be addressed to M.G. (mgoetz@neuro.mpg.de)

Published online: 18 March 2002, DOI: 10.1038/nn828

Radial glial cells, ubiquitous throughout the developing CNS, guide radially migrating neurons and are the precursors of astrocytes. Recent evidence indicates that radial glial cells also generate neurons in the developing cerebral cortex. Here we investigated the role of the transcription factor Pax6 expressed in cortical radial glia. We showed that radial glial cells isolated from the cortex of Pax6 mutant mice have a reduced neurogenic potential, whereas the neurogenic potential of non-radial glial precursors is not affected. Consistent with defects in only one neurogenic lineage, the number of neurons in the Pax6 mutant cortex *in vivo* is reduced by half. Conversely, retrovirally mediated Pax6 expression instructs neurogenesis even in astrocytes from postnatal cortex *in vitro*. These results demonstrated an important role of Pax6 as intrinsic fate determinant of the neurogenic potential of glial cells.

Cell diversity in the vertebrate nervous system is generated through a developmentally regulated cell fate restriction[1,2]. In the cerebral cortex, precursor cells are multipotent at early stages of development[3] and become specified to generate a single cell type at later stages[4,5]. These distinct lineages have been observed under isolated *in vitro* conditions[3,6–8] and show characteristic stereotyped lineage trees[8], implying that cell-intrinsic determinants act as fate-restrictive cues.

The transcription factor Pax6, which is expressed during neurogenesis in the cerebral cortex and is crucial for patterning the telencephalon[9–11], is a possible intrinsic fate determinant. Pax6 is detected specifically in radial glial cells. In *Small-eye* (*Sey*) mice, which lack functional Pax6, these cells have a distorted morphology as well as altered gene expression patterns and cell cycle characteristics[10,12]. As radial glial cells of the cerebral cortex generate neurons *in vitro* and *in vivo*[13–16], we hypothesized that Pax6 might be involved in the neurogenic potential of radial glial cells. We used loss- and gain-of-function approaches to address this question. We show here that the neurogenic progeny of radial glial cells was reduced in the Pax6 mutant cortex, whereas Pax6 transduction enhanced the neuronal lineage and instructed even astrocytes towards neurogenesis.

Results

Reduced neurogenic radial glia in Pax6 mutant

To determine the progeny of radial glial cells in the Pax6 loss-of-function condition, we isolated radial glial cells by fluorescence-activated cell sorting (FACS) using green fluorescent protein (GFP) expression driven by the human GFAP promoter[13,17]. The hGFAP–GFP transgene was crossed into the Pax6 mutant background using *Sey* mice that express a truncated, non-functional form of Pax6 (ref. 18). GFP-positive cells from wild-type and homozygous Pax6 mutant (*Sey/Sey*) littermates were analyzed by FACS (**Fig. 1a–d**). Consistent with previous sorting results, most GFP-positive cells sorted from the cortex of embryonic day (E)14 wild-type and *Sey/Sey* mice were precursors immunoreactive for nestin and the radial glial antigens RC2 and GLAST (**Fig. 1c,d**, gray). In wild-type cortex, sorted radial glial cells were also Pax6 immunoreactive (78 ± 4% of sorted RC2-positive cells, $n = 159$, data not shown). Besides radial glial cells, a relatively high proportion of postmitotic neurons labeled with neuron-specific antiserum against β-tubulin-III was included in the GFP-positive fraction (**Fig. 1c,d**; 2 hours). This most likely was due to the remaining GFP signal in the young neuronal descendants of the sorted radial glia[13]. However, GFP-positive cells were reduced in the Pax6 mutant mice compared to their wild-type littermates (**Fig. 1a,b**; $p < 0.005$, 4 litters). Thus, GFP is targeted to the same populatiozn of GLAST-positive radial glia in Pax6 mutant mice, but their proportion is lower than in wild-type mice. The progeny of the GFP-positive cells sorted from wild-type and *Sey/Sey* cortex was examined after 1 week *in vitro* by double staining with cell-type specific antisera as described previously[13] (see also **Fig. 1** legend). Pax6 mutant radial glia generated a significantly smaller number of pure neuronal clones within 1 week *in vitro* as compared to wild-type littermates (**Fig. 1c,d**; blue fraction; for example, **Fig. 1e,g**). Correspondingly, more non-neuronal clones were generated by the GFP-positive precursors from

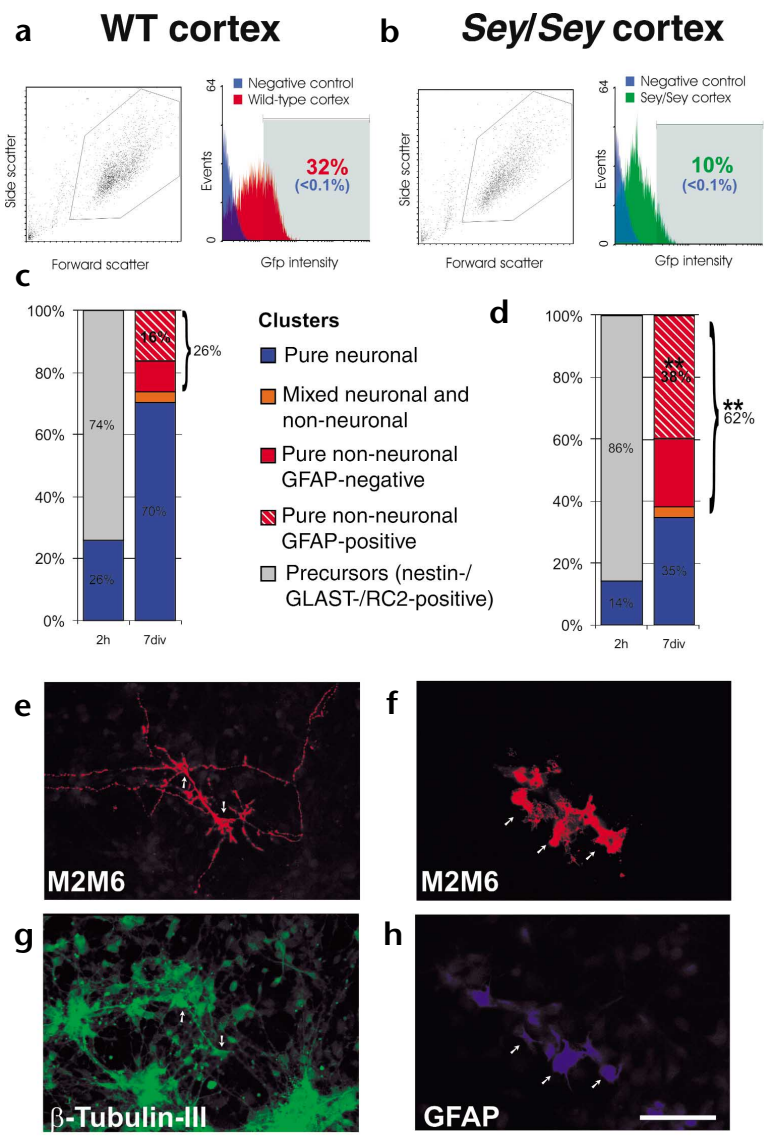

Fig. 1. Progeny of hGFAP–GFP-positive cells from wild-type (WT) and Pax6 mutant cortex. Quantification of the green fluorescent radial glial cells by FACS of the cortex of WT and *Sey/Sey* mice at embryonic day (E) 14, both carrying the transgene GFP under the human GFAP promoter[17]. (**a**,**b**) Left, dot plots of cells in forward scatter and side scatter; polygon indicates the gate selecting the healthy cells. Right, fluorescence intensity versus number of events. Gray, non-transgenic negative control; color, GFP-positive cells; gray squares, sorting gate. The proportion of GFP-positive cells in the *Sey/Sey* cortex (**b**) is one-third that in WT cortex (**a**). (**c**,**d**) Quantification of clusters (identified as shown in **e**–**h**) of sorted cells 2 h or 7 div (days *in vitro*) after sorting from E14 WT (**c**) and *Sey/Sey* (**d**) cortex. Cellular composition of clusters was assessed by immunostaining with cell type-specific antisera. GFP-positive cells from *Sey/Sey* cortex generate few neurons (**d**, blue), increasing from 14% to 35% of clusters from 2 h (left) to 7 div (right), whereas the majority of radial glial cells from WT cortex generate neurons (**c**), increasing from 26% to 70% of clusters between 2 h and 7 div. Number of clusters examined, 487 (2h WT), 318 (7div WT), 632 (2h *Sey/Sey*), 474 (7div *Sey/Sey*); number of GFAP-immunostained clones, 77 (WT), 195 (*Sey/Sey*). Clones containing GFAP-positive cells constitute the same proportion of the non-neuronal clones generated by WT (16% of 26% or 62% of non-neuronal clones) or Pax6 mutant (38% of 62% or 60% of non-neuronal clones). Statistically significant ($p < 0.005$) differences between WT and *Sey/Sey* are indicated by **. (**e**–**h**) Examples of clusters considered as clones. Sorted cells were plated at low density on rat cortical cells, allowing them to be identified by the mouse neural-specific antibodies M2 and M6 on the immuno-negative rat cortical cells. Distinct clusters of M2/M6-immunoreactive cells separated by at least 200 μm were considered as clones derived from individual sorted precursor cells after 1 week *in vitro* (for methodology, see ref. 13). Corresponding fluorescence micrographs (**e**–**h**) showing examples of clones generated by GFP-positive sorted cells from WT (neuronal clone: **e**,**g**) and *Sey/Sey* (glial clone: **f**,**h**) E14 cortex. β-tubulin-III immunoreactivity (green) labels neurons (**g**) and GFAP immunoreactivity (blue) labels astrocytes (**h**). Scale bar, 50 μm.

Sey/Sey cortex (**Fig. 1c**,**d**, red), containing the same relative proportion of GFAP-positive astrocyte clones (hatched, red; examples shown in **Fig. 1f**,**h**).

As the population of the hGFAP–GFP-positive cells was smaller in the Pax6 mutant background, the neurogenic population might have merely lost the GFP signal and therefore be contained in the GFP-negative fraction. Indeed, the hGFAP–GFP-negative fraction from *Sey/Sey* cortex contained more precursor cells than did that from wild-type (wild type, 11 ± 4% nestin-positive cells of all GFP-negative sorted cells, $n = 161$; *Sey/Sey*, 20 ± 5%, $n = 136$). Relatively few cells in the GFP-negative fraction contained Pax6 in wild-type cortex (47% of sorted GFP-negative precursors; $n = 173$). Most cells from the cortex of hGFAP–GFP mice sorted by the lack of green fluorescence were postmitotic neurons, however (NeuN or β-tubulin-III positive). We therefore used the incorporation of bromodeoxyuridine (BrdU; supplied continuously in the culture medium) to discriminate sorted cells that divide *in vitro*—that is, precursors—from the postmitotic neurons included in the sorted fraction. This allowed us to reconstruct the entire progenitor pool of wild-type and Pax6 mutant cortex composed of hGFAP–GFP-positive radial glia and hGFAP–GFP-negative, non-radial glia precursors (**Fig. 2**). One-third of all precursors were GFP negative in E14 wild-type cortex, and they generated neurons only (**Fig. 2a**, gray, hatched). A further third of wild-type cortex precursors were GFP positive and neurogenic (green, hatched), and the last third were GFP-positive and non-neurogenic (green and green with squares, **Fig. 2a**). In the Pax6 mutant progenitor pool, the GFP-negative neurogenic population was still of the same size as in wild-type cortex (**Fig. 2a**,**b**, gray, hatched), whereas the GFP-positive neurogenic population was reduced (green, hatched, **Fig. 2b**). Thus, the GFP-negative fraction does not compensate for the reduced neurogenesis by the GFP-positive fraction. In addition, the GFP-negative precursors of the Pax6 mutant cortex contained a non-neurogenic population generating only immature, nestin-positive precursors that is not detectable in the wild type (white, **Fig. 2b**). Thus, the loss of Pax6 leads to an

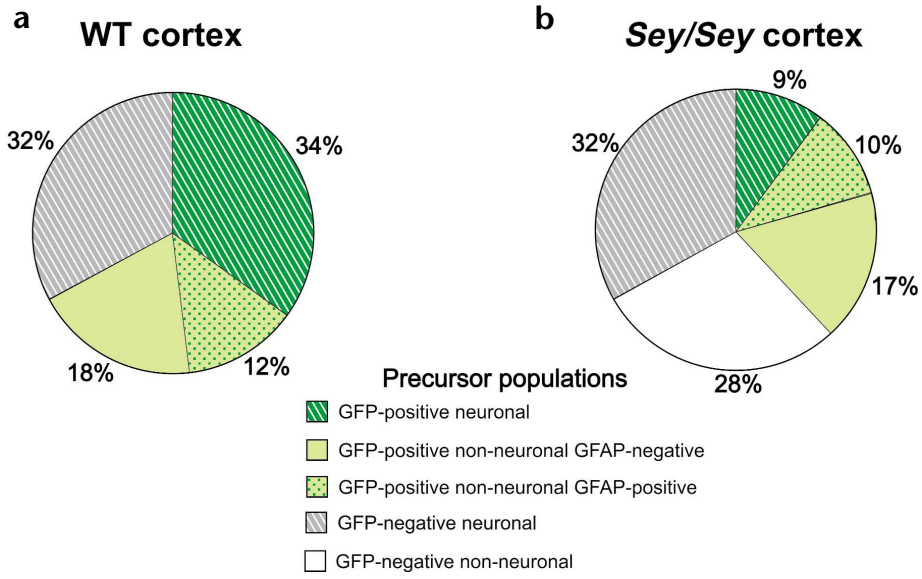

Fig. 2. Composition of the progenitor pool in wild-type (WT) and Pax6 mutant (*Sey*/*Sey*) cortex. (**a**,**b**) Green, hGFAP–GFP-positive precursors; gray, white, hGFAP-negative precursors. Their relative contribution to the progenitor pool was examined by double labeling with the proliferative antigen Ki67 and nestin (see also ref. 34). The clonal progeny of GFP-positive (radial glia) and GFP-negative (non-radial glia) precursors isolated by FACS from WT (**a**) and *Sey*/*Sey* (**b**) cortex containing the hGFAP–GFP transgene was assessed as for the hGFAP–GFP precursors (**Fig. 1**). Pure neuronal clones were taken as indication of neuronal precursors and pure non-neuronal clones as non-neuronal precursors. Populations comprising <5% were omitted for simplicity. Hatching, neurogenic precursor populations; squares, astrocyte precursors. Non-radial glia neurogenic precursors (gray, hatched) are not affected by the loss of Pax6, in contrast to the strong reduction of neurogenic radial glial cells (green, hatched) in the *Sey*/*Sey* cortex. Number of clones analyzed, 318 (WT GFP positive), 288 (WT GFP negative), 474 (*Sey*/*Sey* GFP positive), 236 (*Sey*/*Sey* GFP negative).

increase in immature precursors that have lost their radial glial identity. The non-neurogenic GFP-positive precursors, however, were not affected by the loss of Pax6 and contained the same proportion of astrocyte precursors (green with squares, **Fig. 2**), suggesting that gliogenesis is not affected in the Pax6 mutant cortex (see Discussion).

Neuron reduction in the Pax6 mutant cortex, but not GE

Pax6 mutant cortex and cortical plate are thinner than those of wild type in histological analysis[19]. Moreover, in *Sey*/*Sey* mice, defects in cell adhesion result in different packing density of cells, and abnormal neuronal migration results in ectopic neurons outside the cortical plate[12,20,21]. It is therefore not known whether the proportion of neurons generated in the *Sey*/*Sey* cortex *in vivo* is really reduced, as would be predicted from our *in vitro* fate analysis. To assess this quantitatively, we took advantage of a transgenic mouse line in which neurons can be readily visualized by the expression of GFP. The Tau:GFP mouse line expresses a GFP cDNA from the Tau locus, which results in labeling of all neurons shortly after birth[22]. The analysis of GFP-positive cells from wild-type and *Sey*/*Sey* littermate cortices (each containing one GFP allele) confirmed localization of the GFP transgene product in neurons (**Fig. 3a**,**b**, Methods). Quantification of green fluorescent neurons by FACS showed a prominent reduction of Tau:GFP-positive neurons in *Sey*/*Sey* compared to wild-type cortex at E14 (**Fig. 3c**,**d**; significant, $p < 0.005$, 4 litters). The number of neurons was still reduced at E16 (mean reduction to 67 ± 3% of wild-type cortex), whereas no significant difference was found between the ganglionic eminence (GE) of *Sey*/*Sey* and wild-type mice (**Fig. 3e**,**f**). Thus, the decrease in the overall neuronal numbers in the *Sey*/*Sey* cortex *in vivo* was restricted to the former Pax6-positive territory and did not result from a delay of differentiation, as it persists into late embryonic stages.

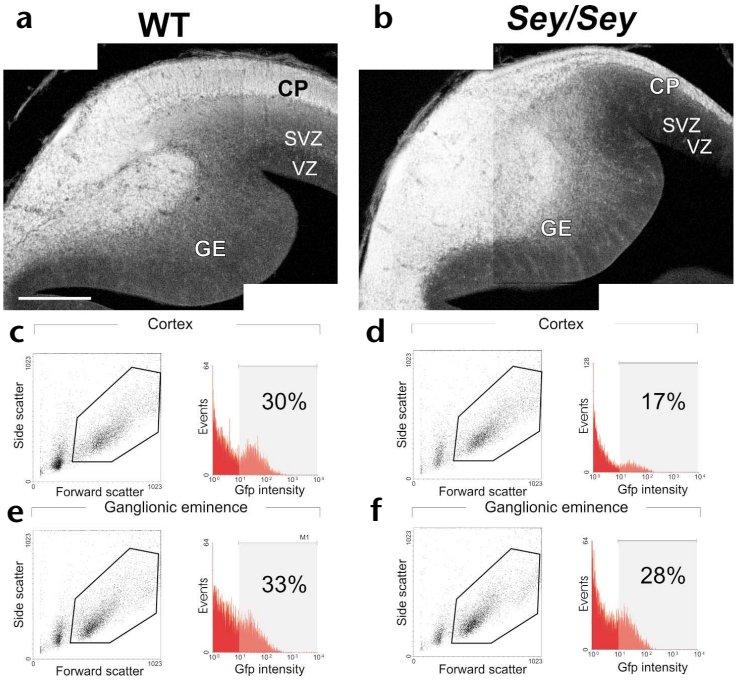

Fig. 3. Reduction of neurons in the Pax6 mutant cortex, but not GE, *in vivo*. (**a**,**b**) Sections of the telencephalon from E14 wild-type (WT) (**a**) and *Sey*/*Sey* (**b**) mice both carrying the GFP transgene in the Tau locus[22]. Postmitotic neurons are green fluorescent and appear white in the section. Note that the cortical plate (CP) is thinner in the *Sey*/*Sey* (**b**) cortex than in the WT (**a**), whereas the ganglionic eminence (GE) seems not affected. Ventricular zone (VZ) and subventricular zone (SVZ) are indicated. Scale bar, 200 μm. (**c**–**f**) Fluorescent profiles (as in **Fig. 1**) from E14 mice carrying one *GFP* allele. The proportion of the green fluorescent neurons from the *Sey*/*Sey* cortex (**d**) is half that in the WT cortex (**c**), but no difference is detectable in the GE of WT (**e**) and mutant (**f**).

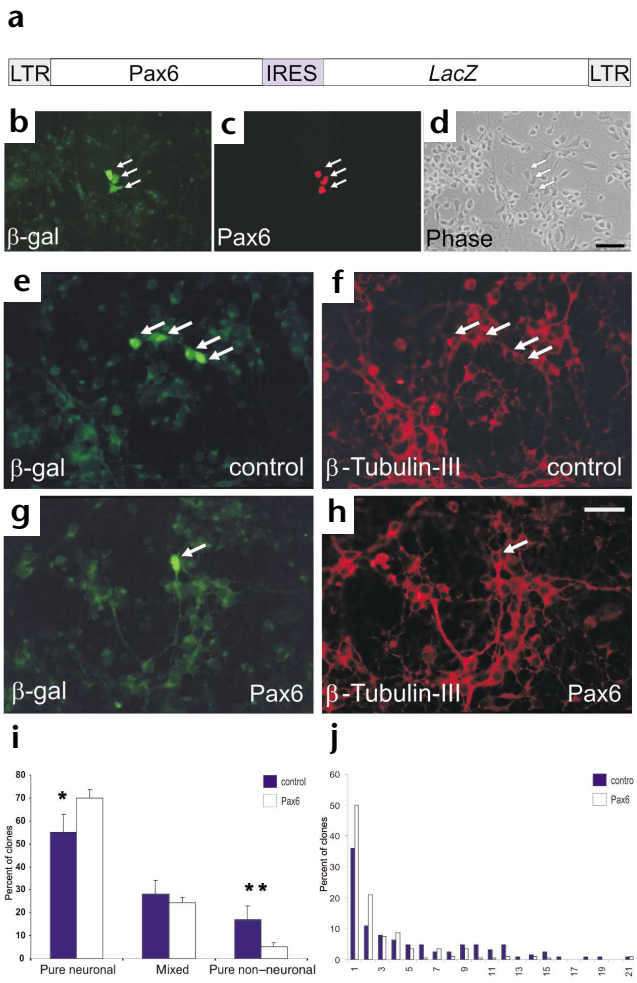

Fig. 4. Pax6 transduction increases neurogenesis in precursors from embryonic cortex. The retroviral vector (**a**) allows co-expression of *lacZ* and Pax6 cDNA in corresponding micrographs of a β-galactosidase- (**b**) and Pax6-immunoreactive (**c**) cluster of cells from GE of *Sey*/*Sey* mice at E14 that do not contain endogenous Pax6. Compare with the corresponding phase contrast micrograph in (**d**); scale bar, 25 μm. All β-galactosidase-positive cells contained high levels of Pax6 protein when double stained with Pax6 antiserum 3 d after infection with the Pax6 vector (arrows). (**e**–**h**) Corresponding fluorescence micrographs show β-galactosidase-positive cells (**e**,**g**) from E14 WT cortex transduced with control (**e**,**f**) or Pax6 (**g**,**h**) virus double stained with the neuron-specific antibody against β-tubulin-III (**f**,**h**) after 7 d *in vitro*. Arrows, double-positive cells; scale bar, 12.5 μm. (**i**) Histogram of cell type analysis of clones from E14 WT cortex infected with the control (dark bars) or Pax6 virus (light bars) after 7 d *in vitro* (*y* axis indicates the percentage of clones). Note that pure neuronal clones increase at the expense of pure non-neuronal clones after Pax6 transduction. Number of clones analyzed, 461 (control); 1,016 (Pax6). *, $p < 0.01$; **, $p < 0.005$. (**j**) Size distribution of clones generated by control (dark bars) and Pax6 (light bars) infected cortical precursor cells from E14 WT after 5–7 d *in vitro*. The *x* axis indicates the clone size as numbers of cells per clone and the *y* axis the frequency of clones in percent. Note the strong increase in the number of single cell clones at the expense of larger clones after Pax6 transduction. Number of clones analyzed, 811 (control), 983 (Pax6).

Viral Pax6 transduction in cells from embryonic cortex

These results suggested that Pax6 maintains or directs neurogenesis in the cerebral cortex. To test for an instructive role of Pax6 directly, we performed gain-of-function experiments using a replication-incompetent retroviral vector containing full-length Pax6 cDNA and the marker gene *lacZ* (**Fig. 4a**). Dissociated cells from E14 cortex were infected shortly after plating and analyzed by double immunocytochemistry 2–7 days after infection. Reliable co-expression of the marker β-galactosidase and the Pax6 protein was seen (**Fig. 4b–d**), and virally transduced cells showed fluorescent Pax6 immunoreactivity 3.6-fold higher than that from endogenous Pax6 in cortical cells (see also ref. 23 and Methods). As the retroviral genome incorporates stably into the genome of infected precursor cells (two-thirds of which are GLAST-positive radial glia), all the progeny inherit the viral genome containing the marker gene *lacZ*. A low titer of retrovirus (about 5×10^4) infects only few precursor cells (fewer than 25 per coverslip), and their progeny are detectable as distinct clusters of β-galactosidase-positive cells surrounded by negative cells after 7 days *in vitro* (**Fig. 4b**,**e**,**g**). Cell type analysis of β-galactosidase-positive clusters (**Fig. 4e–h**) showed a significant ($p < 0.01$) increase in pure neuronal and a corresponding decrease in pure non-neuronal clones after Pax6 transduction (**Fig. 4i**). Although the frequency of mixed clones was not affected, they contained more neurons after Pax6 transduction (60% of β-galactosidase-immunoreactive cells in mixed Pax6-transduced clones were neurons compared to 40% in the control; $p < 0.005$).

Pax6 transduction also affected cell proliferation, resulting in a higher proportion of clones containing only a single cell (**Fig. 4j**). Single-cell clones are due to the integration of the viral genome into only one daughter cell after replication[24], which remains as a single cell if it stops proliferating. Accordingly, almost all single-cell clones are postmitotic neurons[23]. Thus, some Pax6-transduced precursors stopped proliferating immediately and differentiated into neurons. In addition, Pax6 transduction provoked an increase of neuronal precursors, as neurogenesis was doubled in clones containing more than one cell; 31% of control-infected clones with more than one cell are pure neuronal ($n = 235$) as compared with 62% of the Pax6-infected clones ($n = 214$; $p < 0.005$). The opposite phenotype, an

Table 1. Mean size of clones from Pax6- and control-transduced wild-type and *Sey*/*Sey* precursor cells

Cell type	Virus	Clone size	s.e.m.	No. of clones
Telencephalon precursor cells				
WT cortex (E14)	Control	5.8	0.6	811
WT cortex (E14)	Pax6	3.0**	0.3	983
Sey/*Sey* cortex (E14)	Control	7.4*	0.7	520
Sey/*Sey* cortex (E14)	Pax6	2.7**	0.1	159
WT GE (E14)	Control	5.2	0.8	514
WT GE (E14)	Pax6	5.0	0.9	226
Postnatal astrocytes				
WT cortex (P3-11)	Control	2.7	0.25	36
WT cortex (P3-11)	Pax6	1.8**	0.17	30

A significant decrease occurs in the size of clones generated by Pax6-transduced cells from the cortex of both wild-type (WT) and *Sey*/*Sey* and by Pax6-transduced postnatal astrocytes, but there is no effect in cells from the GE. In contrast, the clone size of Pax6-deficient *Sey*/*Sey* cortical precursors is increased compared to WT cortex. Significant differences to WT cortex infected with control virus are indicated (*, $p < 0.01$; **, $p < 0.005$).

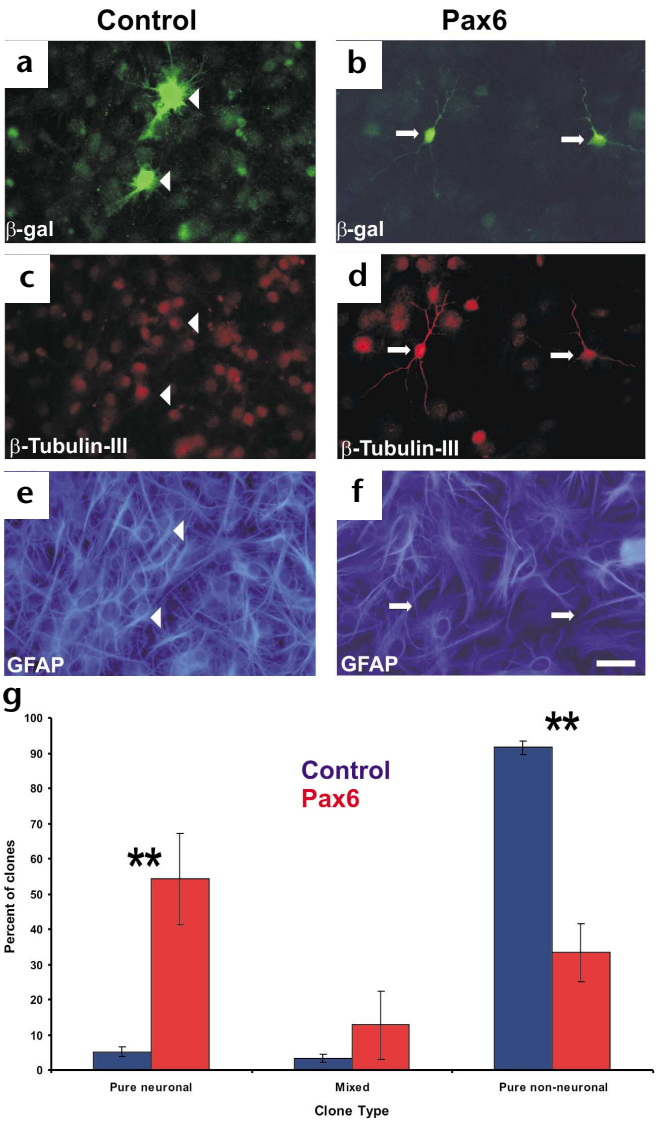

Fig. 5. Pax6 directs astrocytes towards neurogenesis. (**a**–**f**) Corresponding fluorescence micrographs (**a**,**c**,**e**; **b**,**d**,**f**) show β-galactosidase-positive cells (**a**,**b**) after 7 d in chemically defined medium generated from astrocytes of postnatal cortex transduced with the control (**a**,**c**,**e**) or Pax6 virus (**b**,**d**,**f**). Cells were double stained with cell-type specific markers for neurons (**c**,**d**) or astrocytes (**e**,**f**). Arrowheads depict an example of an astroglial clone (**a**,**c**,**e**) and arrows (**b**,**d**,**f**) depict an example of a two-cell neuronal clone generated by astrocytes infected with the Pax6 virus. (**g**) Histogram depicts the quantification of clone types generated by astrocytes from postnatal cortex infected with the control virus BAG (blue bars) or the Pax6 virus (red bars) after 7 d *in vitro*. Pure neuronal clones increase at the expense of pure non-neuronal clones after Pax6 transduction. Number of clones analyzed, 324 (control), 67 (Pax6). **, $p < 0.005$. Scale bar, 25 μm.

increased clone size, was seen in cultures from *Sey*/*Sey* cortex (**Table 1**). This phenotype was reversed by Pax6 transduction (**Table 1**), consistent with a cell-autonomous function of Pax6 in neurogenesis and cell proliferation.

Pax6 induces neurogenesis in astrocytes

Our results showed that Pax6 affects neurogenesis in embryonic cortical precursors isolated during the period of neurogenesis. To examine whether Pax6 can also instruct neurogenesis in cells beyond the phase of neurogenesis, we forced Pax6 expression in Pax6-negative astrocytes[12,25] (see **Supplementary Fig. 1** on the supplementary information page of *Nature Neuroscience* online) isolated from postnatal cerebral cortex more than 1 week after neurogenesis (see Method for culture conditions). When control clones were examined 7 days after infection, a minor fraction had turned into pure neuronal clones (**Fig. 5**). This low degree of neurogenesis was consistent with previous results[26,27] and was most likely due to contamination with astrocytes from the adult subventricular zone (SVZ) that act as stem cells[27,28]. In contrast, more than half of GFAP-positive cells infected with Pax6-encoding virus generated clones containing exclusively β-tubulin-III-positive neurons (**Fig. 5**). The β-tubulin-III-positive cells also contained NeuN, another neuron-specific protein[29], and were immunoreactive to GABA or glutamate (data not shown), suggesting that these cells were indeed neurons. As seen with cells from embryonic cortex, Pax6 transduction of astrocytes also affected their proliferation and resulted in a smaller clone size (**Table 1**).

Pax6 influences bHLH transcription factors

The prominent neurogenic effect of Pax6 raises the question how Pax6 interacts with transcription factors of the bHLH family that have important roles in neurogenesis[30,31]. We therefore examined neurogenin (Ngn) 1 and 2, Mash1 and Olig2 in Pax6 loss-of-function and gain-of-function experiments (**Fig. 6**). Consistent with previous results obtained by *in situ* hybridization[11,32], we found a marked reduction of Ngn2 protein (and less pronounced reduction of Ngn1, data not shown) in the *Sey/Sey* cortex (**Fig. 6a**,**b**). Similar to Mash1, Olig2 is restricted in its expression to the GE in wild-type mice[33] and expands ectopically into the Pax6 mutant cortex (**Fig. 6c**,**d**). In gain-of-function experiments, the opposite phenotype was seen. After Pax6-transduction, more cells from E14 cortex were Ngn2 immunoreactive and fewer contained Mash1 as compared to control infected cells (**Fig. 6e**). No change was seen for Ngn1, and no Olig2-immunoreactive cells were detected in control or Pax6-infected cortical cultures (data not shown). GFAP-immunoreactive astrocytes from postnatal cortex differed in their bHLH expression pattern in that most of them contained Mash1 and Olig2, but not Ngn2 (**Fig. 6f**). Mash1 was downregulated upon Pax6 transduction and there was a similar trend for Olig2 (**Fig. 6f**), whereas Ngn2 immunoreactivity was not induced (data not shown).

Discussion

Pax6 is required for one of two neurogenic lineages

Our results showed that Pax6 directs astroglial cells towards neurogenesis in embryonic and postnatal cerebral cortex. The Pax6-dependent neurogenic lineage in embryonic cortex most likely corresponds to the recently discovered neurogenic population of radial glial cells[13–16]. First, Pax6 is localized in cells with radial glial properties such as RC2 and GLAST immunoreactivity and hGFAP–GFP expression[13,34]. Second, only the neurogenic progenitor population with radial glial properties is affected by the loss of Pax6 function, whereas the neurogenic population of the GFP-negative precursors remains normal. These data are also in line with our previous results on cell-autonomous defects in radial glia morphology in the Pax6-mutant cortex[10] (also ref. 20). The wild-type environment *in vitro* is not able to rescue the reduction of the neurogenic population after the loss of Pax6

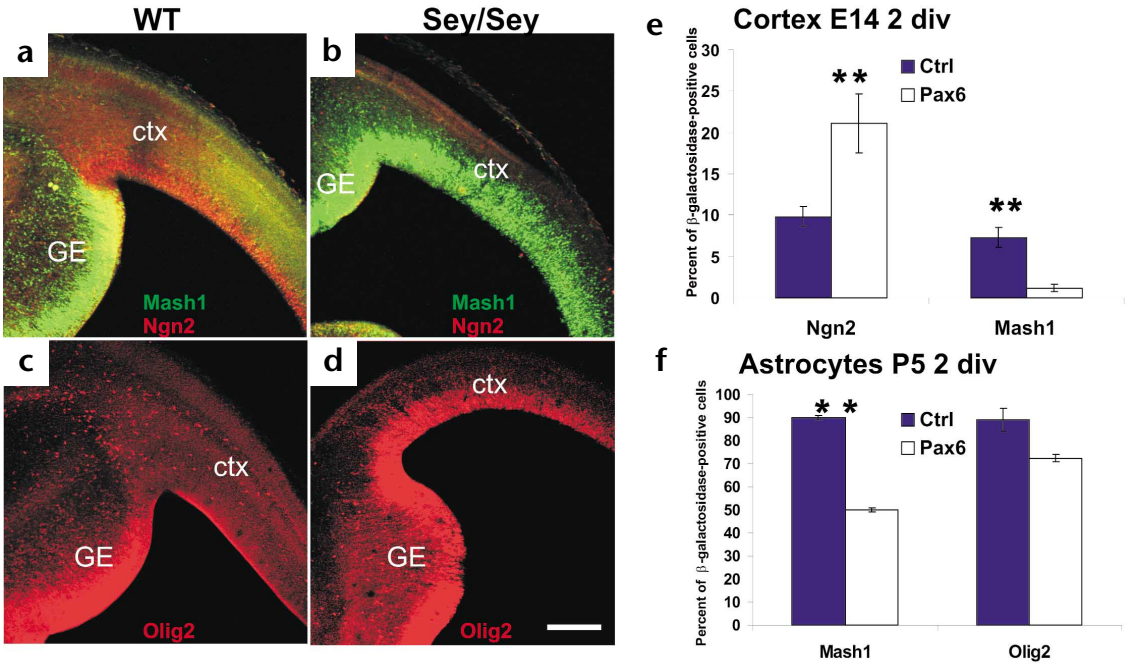

Fig. 6. Pax6 regulates bHLH transcription factors. (**a**–**d**) shows micrographs of sections from E14 wild-type (WT; **a**,**c**) and *Sey/Sey* (**b**,**d**) telencephalon stained with the antisera indicated. Ngn2 immunoreactivity is lost, whereas Mash1 and Olig2 staining is increased in the *Sey/Sey* cortex. Scale bar, 200 μm. (**e**,**f**) Percentage of β-galactosidase-positive cells in dissociated cell cultures from E14 cortex infected at the time of plating (**e**) or P5 astrocyte cultures infected after the first passage (**f**) that are immunopositive for the bHLH transcription factors indicated. Cultures were fixed 2 d after infection with the control (dark bars) or the Pax6 virus (light bars). Overexpression of Pax6 has regulatory effects opposite to those of the loss of Pax6 function in *Sey/Sey* cortex, namely upregulation of Ngn2 and downregulation of Mash1 or Olig2. Number of clones analyzed (**e**,**f**), Mash1, 82 (BAG), 132 (Pax6); Olig2, 336 (BAG), 172 (Pax6). **, $p < 0.005$.

function, and Pax6 transduction of relatively few precursors results in an increase in the neurogenic lineage. Pax6 therefore seems to be a crucial intrinsic determinant for neurogenic fate of cortical radial glia precursors.

Pax6 directs multipotent precursors to neurogenesis

Although neuronal progenitors were less prevalent in the absence of Pax6, we saw a converse increase in non-neuronal progenitors that did not generate GFAP-positive astrocytes, but rather remained as immature precursors in dissociated cell cultures without the addition of growth factors. In neurosphere cultures, however, Pax6 mutant cortex cells generate more neurospheres than do wild-type cortex cells (see **Supplementary Fig. 2** on the supplementary information page of *Nature Neuroscience* online), implying an increase in multipotent precursors in the absence of Pax6. These *in vitro* data therefore suggest that Pax6 effects the transition of an immature precursor to a neuron-restricted progenitor rather than acting as a neuron–glia fate switch. Indeed, in contrast to the premature astrocyte differentiation in the cortex of *Ngn2;Mash1* double mutant mice[30], astrocyte differentiation is normal in the *Sey/Sey* cortex as assessed by the markers GFAP, TN-C, S100β and synemin (data not shown; also ref. 12). Notably, the two mutants share the phenotype of an early increase in SVZ precursors, namely cells that undergo cytokinesis in the parenchyma[12,19,20,30,35]. SVZ precursors do not contain the radial glial marker GLAST[36]. Therefore, the enlarged SVZ of *Sey/Sey* mice should contain the increased population of GFP-and GLAST-negative precursors consisting of the abnormal, potentially multipotent subpopulation. Consistent with immaturity of these precursors, we did not observe neurons in the SVZ as detected in ref. 20 (**Fig. 3a**,**b** and data not shown). Indeed, alterations in gene expression occur in the Pax6 mutant SVZ[35]. The SVZ phenotype of Pax6 mutant mice is particularly intriguing in light of the SVZ location of stem cells at later developmental stages, and implies that Pax6 may be a simultaneous negative regulator of stem cell and SVZ fate.

Pax6 is a potent neurogenic gene

The gain-of-function experiments show a prominent neurogenic effect even in astrocytes from postnatal cortex. To our knowledge, this effect is so far unique. Extrinsic stimuli exert only a weak neurogenic effect on astrocytes, consistent with a low degree of contamination of stem cells from the adult SVZ[26–28]. The transduction of astrocytes with transcription factors known for their neurogenic role in development, namely members of the bHLH proneural transcription factor family, yields hardly any or no neurogenesis[31,37]. Although Ngn1 is able to induce a neurogenic fate in precursors from embryonic cortex, only GFAP levels are reduced and morphology is changed in astrocytes[31]. Thus, both Pax6 and Ngn1 enhance neurogenesis in embryonic precursors, but only Pax6 initiates the complete neurogenic program in astrocytes. Ngn1 might be responsible for the neurogenic lineage generated by non-radial glial precursors not affected in the Pax6 mutant cortex. This would be consistent with the failure of Pax6 to regulate Ngn1 in gain-of-function experiments and with the remaining Ngn1-expression in the Pax6 mutant cortex. In contrast, Pax6 positively regulates Ngn2 (see also refs. 38,39) but negatively affects Mash1 in embryonic and astrocyte precursors. As Mash1 is not able to rescue a decrease of neurogenesis in the embryonic cortex[40] (see also data above), it might have other

than positive neurogenic roles in the cortex. Notably, Mash1 is upregulated by Pax6 in the retina, where Pax6 directs multipotent fate[38]. This could explain the opposite phenotype of Pax6 mutation in the retina (loss of multipotent precursors and decreased proliferation)[38] and the cortex (increased proliferation[10] and multipotent precursors; **Supplementary Figure 2**). Thus the combinatorial network of bHLH transcription factors might implement the close link between patterning and cell fate in vertebrate CNS[41].

Implications for neuronal replacement

Our results indicate that in the cerebral cortex, Pax6 seems to function primarily in cells with astroglial traits during development and postnatal stages. Besides radial glial cells generating neurons[13–16], cells with astroglial traits are responsible for the neurogenesis in the two regions of the adult mammalian CNS that continue to generate neurons[28,42]. Moreover, expanded glial cultures from the embryonic GE generate region-specific neuronal subtypes[16]. This evidence suggests a general role of cells with astroglial features as neuronal precursor cells, and our results implicate Pax6 as a crucial neurogenic determinant in these cells. As Pax6-transduced astrocytes were able to generate neurons *in vitro*, the loss of Pax6 expression in most astrocytes of the adult CNS might be one reason for the loss of their neurogenic lineage. These data are therefore a crucial step in the identification of the molecular signals able to reinitiate the former neurogenic potential in astrocytes, and may help make it possible to use the most abundant cell type in the mammalian CNS to replace degenerating neurons.

Methods

Mice. The *Small-eye* (*Sey)* allele[18] was maintained in a C57BL/6J × DBA/2J background, the 94-4 transgenic mouse line[17] in a FVB/N background and the Tau:GFP mice[22] in a C57BL/6J background. Neuronal localization of Tau:GFP was confirmed in embryonic cortex (98% of GFP-positive cells were immunoreactive to β-tubulin-III in wild-type and *Sey/Sey*; n = 292). To obtain *Sey/Sey* homozygous embryos carrying one GFP transgene, we crossed F1 mice (matings of *Sey*/+ with the respective transgenic line) with non-transgenic *Sey*/+ mice. Retroviral experiments were done with C57BL/6J mice; the feeder layer for the sorting experiments was prepared from Wistar rats. The day of vaginal plug was considered as embryonic day 0 (E0) and the day of birth as postnatal day 0 (P0).

FACS. At least 10,000 events of healthy cells were analyzed with a FACSort (Becton Dickinson, Franklin Lakes, New Jersey) at a flow rate of <2,500 cells/s. For sorting, the single cell mode and a sort rate between 50 and 150 cells/s was used with sorting gates for the GFP-positive cells defined as containing less than 0.5% signals of the negative control (that is, non-fluorescent cells; **Fig. 1a**,**b**). Fewer than 100 cells sorted from mouse cortex were cultured with an excess of rat cortical cells, allowing the identification of individual sorted cells and their progeny by the mouse-specific antibodies M2M6. For further details, see ref. 13.

Cell culture. High-density dissociated cell cultures from embryonic cortex or astrocyte cultures from postnatal cortex were described previously[13,34]. Astrocytes from cortex of P5–11 mice were cultured in Dulbecco's modified Eagle medium (DMEM) with 10% fetal calf serum (FCS) and, in some experiments, 10 ng/ml EGF and FGF2. After 7–10 d, cells were passaged, plated onto poly-D-lysine-coated glass coverslips at a density of 1×10^5 cells per well and infected with retroviral vectors (below), then switched the next day to chemically defined medium (B27, Gibco-BRL, Paisley, UK). Purity of these cultures was confirmed by immunocytochemistry; 90 ± 2% (n = 235) of all cells were GFAP positive, 2 ± 2% (n = 235) β-tubulin-III positive, 3 ± 3% (n = 150) O4 positive and 4 ± 4% (n = 26) fibronectin positive. The identity of retrovirally infected cells was assessed at the earliest possible time point (2 d after infection) and 99 ± 1% of control (n = 131) and 86 ± 1% of Pax6 cells (n = 161) were GFAP positive. The slight reduction in GFAP in Pax6 virus–infected cells might be the start of transformation into neurons.

Retroviral transduction. A 783-bp fragment containing the entire coding sequence of Pax6 was inserted in the sense orientation into the *Bgl*II unique restriction site of the retroviral vector 1704, between the upstream LTR and the EMC IRES sequence (gift of J.E. Majors[43]). BOSC 23 helper-free packaging cells were used for viral production[44]. Cells were infected 2 h after plating at a concentration giving not more than 25 clones per coverslip, resulting in a 2.8% probability of clonal superimposition for the average diameter (300 μm) of control-transduced clones, which are larger than Pax6-transduced clones. Digital pictures of the Pax6 immunoreactivity were obtained with a Zeiss (Oberkochen, Germany) Axiocam color camera and analyzed with ImageJ 1.23y software (National Institutes of Health, Bethesda, Maryland). The intensity of Pax6 signal of β-galactosidase-positive cells was measured in relation to the Pax6 intensity of β-galactosidase-negative cells in the same culture.

Immunostaining. Cells or brains were fixed with 2-4% paraformaldehyde and vibratome sections were prepared as described in[34]. We used the mouse monoclonal antibody (mAb) against nestin (rat 401, IgG1; 1:4; Developmental Studies Hybridoma Bank, Iowa City, Iowa), mAb against GFAP (IgG1; 1:200; Sigma, St. Louis, Missouri), mAb against β-tubulin-III (IgG2b; 1:100; Sigma), mAB against NeuN (IgG1; 1:50; Chemicon, Temecula, California), mAb against O4 (IgM, 1:100; ref. 45), the rabbit polyclonal antiserum (pAb) against fibronectin (1:100; Life Technologies, Rockville, Maryland), pAb against GLAST (1:8,000; Chemicon), mAb against RC2 (IgM, 1:500; provided by P. Leprince; ref. 34), mAb against BrdU (IgG1; 1:10; Bio-Science Product, Emmenbruecke, Switzerland), the rat mAbs M2 and M6 (rat, 1:200, provided by C. Lagenaur; ref. 13), pAb against Pax6 (1:500; BABCO, Richmond, California), pAb against Ngn1 (1:500, provided by F. Guillemot; ref. 46), pAb against Ngn2 (1:300; ref. 47), pAb against Olig2 (1:400; ref. 33), mAb against Mash1 (1:2, provided by D. Anderson; ref. 48), pAb (O3G, 1:500, provided by J. Price; ref. 45) or mAb against β-galactosidase (IgG2a; 1:2,000; Promega, Madison, Wisconsin) and pAb against GFP (1:2,000; Chemicon), following standard protocols, with secondary antisera from Europath (Cornwall, UK). Specimen were mounted in Aqua Poly/Mount (Polysciences, Northampton, UK) and analyzed using a Zeiss Axiophot or Leica Microsystems (Heidelberg, Germany) confocal fluorescence microscope.

Data analysis. Data were tested for significance by Student's t-test. For cell fate analysis, the proportion of neuronal, mixed and non-neuronal clones was analyzed for each coverslip and means were calculated from different coverslips. Data are derived from 2–7 different experimental batches containing at least 12 different coverslips.

Note: Supplementary information is available on the Nature Neuroscience website.

Acknowledgements

We are grateful to A. Stoykova and A. Messing for the Sey- and 94-4 mice, respectively; D. Anderson, F. Guillemot, C. Lagenaur, P. Leprince and J. Price for antisera; J.E. Majors for the viral backbone plasmid; H. Wekerle and W. Klinkert for access to the FACSort; M. Öcalan for expertise in tissue culture; and F. Guillemot, B. Grothe, M. Korte and R. Klein for comments on the manuscript. The monoclonal antibody against nestin was obtained from the Developmental Studies Hybridoma Bank. Our work was supported by the EU Grant QLK3-1999-00894, European Cell Therapy in the Nervous System, a Marie Curie Fellowship to P.M. and the Max-Planck Society. F.C. is an Assistant Telethon Scientist (grant 38/CP).

Competing interests statement

The authors declare that they have no competing financial interests.

RECEIVED 23 JANUARY; ACCEPTED 19 FEBRUARY 2002

1. Anderson, D.J. The neural crest cell lineage problem: neuropoiesis? *Neuron* **3**, 1–12 (1989).
2. Lillien, L. Neural development: instructions for neural diversity. *Curr. Biol.* **7**, R168–R171 (1997).
3. Williams, B.P. & Price, J. Evidence for multiple precursor cell types in the embryonic rat cerebral cortex. *Neuron* **14**, 1181–1188 (1995).
4. Grove, E.A. *et al.* Multiple restricted lineages in the embryonic rat cerebral cortex. *Development* **117**, 553–561 (1993).
5. Reid, C.B., Liang, I. & Walsh, C. Systematic widespread clonal organization in cerebral cortex. *Neuron* **15**, 299–310 (1995).
6. Qian, X. *et al.* Timing of CNS cell generation: a programmed sequence of neuron and glial cell production from isolated murine cortical stem cells. *Neuron* **28**, 69–80 (2000).
7. Luskin, M.B., Pearlman, A.L. & Sanes, J.R. Cell lineage in the cerebral cortex of the mouse studied *in vivo* and *in vitro* with a recombinant retrovirus. *Neuron* **1**, 635–647 (1988).
8. Qian, X., Goderie, S.K., Shen, Q., Stern, J.H. & Temple, S. Intrinsic programs of patterned cell lineages in isolated vertebrate CNS ventricular zone cells. *Development* **125**, 3143–3152 (1998).
9. Walther, C. & Gruss, P. Pax-6, a murine paired box gene, is expressed in the developing CNS. *Development* **113**, 1435–1449 (1991).
10. Götz, M., Stoykova, A. & Gruss, P. Pax6 controls radial glia differentiation in the cerebral cortex. *Neuron* **21**, 1031–1044 (1998).
11. Stoykova, A., Treichel, D., Hallonet, M. & Gruss, P. Pax6 modulates the dorsoventral patterning of the mammalian telencephalon. *J. Neurosci.* **20**, 8042–8050 (2000).
12. Stoykova, A., Götz, M., Gruss, P. & Price, J. Pax6-dependent regulation of adhesive patterning, R-cadherin expression and boundary formation in developing forebrain. *Development* **124**, 3765–3777 (1997).
13. Malatesta, P., Hartfuss, E. & Götz, M. Isolation of radial glial cells by fluorescent-activated cell sorting reveals a neuronal lineage. *Development* **127**, 5253–5263 (2000).
14. Noctor, S.C., Flint, A.C., Weissman, T.A., Dammerman, R.S. & Kriegstein, A.R. Neurons derived from radial glial cells establish radial units in neocortex. *Nature* **409**, 714–720 (2001).
15. Miyata, T., Kawaguchi, A., Okano, H. & Ogawa, M. Asymmetric inheritance of radial glial fibers by cortical neurons. *Neuron* **31**, 727–741 (2001).
16. Skogh, C. *et al.* Generation of regionally specified neurons in expanded glial cultures derived from the mouse and human lateral ganglionic eminence. *Mol. Cell Neurosci.* **17**, 811–820 (2001).
17. Zhuo, L. *et al.* Live astrocytes visualized by green fluorescent protein in transgenic mice. *Dev. Biol.* **187**, 36–42 (1997).
18. Hill, R.E. *et al.* Mouse Small eye results from mutations in a paired-like homeobox-containing gene. *Nature* **354**, 522–525 (1991).
19. Schmahl, W., Knoedlseder, M., Favor, J. & Davidson, D. Defects of neuronal migration and the pathogenesis of cortical malformations are associated with *Small eye* (*Sey*) in the mouse, a point mutation at the *Pax-6* locus. *Acta Neuropathol. (Berl.)* **86**, 126–135 (1993).
20. Caric, D., Gooday, D., Hill, R.E., McConnell, S.K. & Price, D.J. Determination of the migratory capacity of embryonic cortical cells lacking the transcription factor Pax-6. *Development* **124**, 5087–5096 (1997).
21. Chapouton, P., Gärtner, A. & Götz, M. The role of Pax6 in restricting cell migration between developing cortex and basal ganglia. *Development* **126**, 5569–5579 (1999).
22. Tucker, K.L., Meyer, M. & Barde, Y.A. Neurotrophins are required for nerve growth during development. *Nat. Neurosci.* **4**, 29–37 (2001).
23. Heins, N. *et al.* Emx2 promotes symmetric cell divisions and a multipotential fate in precursors from the cerebral cortex. *Mol. Cell Neurosci.* **18**, 485–582 (2001).
24. Hajihosseini, M., Iavachev, L. & Price, J. Evidence that retroviruses integrate into post-replication host DNA. *EMBO J.* **12**, 4969–4974 (1993).
25. Stoykova, A., Fritsch, R., Walther, C. & Gruss, P. Forebrain patterning defects in Small eye mutant mice. *Development* **122**, 3453–3465 (1996).
26. Hildebrand, B., Olenik, C. & Meyer, D.K. Neurons are generated in confluent astroglial cultures of rat neonatal neocortex. *Neuroscience* **78**, 957–966 (1997).
27. Laywell, E.D., Rakic, P., Kukekov, V.G., Holland, E.C. & Steindler, D.A. Identification of a multipotent astrocytic stem cell in the immature and adult mouse brain. *Proc. Natl. Acad. Sci. USA* **97**, 13883–13888 (2000).
28. Doetsch, F., Caille, I., Lim, D.A., Garcia-Verdugo, J.M. & Alvarez-Buylla, A. Subventricular zone astrocytes are neural stem cells in the adult mammalian brain. *Cell* **97**, 703–716 (1999).
29. Mullen, R.J., Buck, C.R. & Smith, A.M. NeuN, a neuronal specific nuclear protein in vertebrates. *Development* **116**, 201–211 (1992).
30. Nieto, M., Schuurmans, C., Britz, O. & Guillemot, F. Neural bHLH genes control the neuronal versus glial fate decision in cortical progenitors. *Neuron* **29**, 401–413 (2001).
31. Sun, Y. *et al.* Neurogenin promotes neurogenesis and inhibits glial differentiation by independent mechanisms. *Cell* **104**, 365–376 (2001).
32. Toresson, H., Potter, S.S. & Campbell, K. Genetic control of dorsal–ventral identity in the telencephalon: opposing roles for Pax6 and Gsh2. *Development* **127**, 4361–4371 (2000).
33. Takebayashi, H. *et al.* Dynamic expression of basic helix-loop-helix Olig family members: implication of Olig2 in neuron and oligodendrocyte differentiation and identification of a new member, Olig3. *Mech. Dev.* **99**, 143–148 (2000).
34. Hartfuss, E., Galli, R., Heins, N. & Götz, M. Characterization of CNS precursor subtypes and radial glia. *Dev. Biol.* **229**, 15–30 (2001).
35. Tarabykin, V., Stoykova, A., Usman, N. & Gruss, P. Cortical upper layer neurons derive from the subventricular zone as indicated by Svet1 gene expression. *Development* **128**, 1983–1993 (2001).
36. Estivill-Torrus, G., Pearson, H., van Heyningen, V., Price, D.J. & Rashbass, P. Pax6 is required to regulate the cell cycle and the rate of progression from symmetrical to asymmetrical division in mammalian cortical progenitors. *Development* **129**, 455–466 (2002).
37. Farah, M.H. *et al.* Generation of neurons by transient expression of neural bHLH proteins in mammalian cells. *Development* **127**, 693–702 (2000).
38. Marquardt, T. *et al.* Pax6 is required for the multipotent state of retinal progenitor cells. *Cell* **105**, 43–55 (2001).
39. Scardigli, R., Schuurmans, C., Gradwohl, G. & Guillemot, F. Crossregulation between Neurogenin2 and pathways specifying neuronal identity in the spinal cord. *Neuron* **31**, 203–217 (2001).
40. Fode, C. *et al.* A role for neural determination genes in specifying the dorsoventral identity of telencephalic neurons. *Genes Dev.* **14**, 67–80 (2000).
41. Götz, M. How are neurons specified: master or positional control? *Trends Neurosci.* **21**, 135–136 (1998).
42. Seri, B., Garcia-Verdugo, J.M., McEwen, B.S. & Alvarez-Buylla, A. Astrocytes give rise to new neurons in the adult mammalian hippocampus. *J. Neurosci.* **21**, 7153–7160 (2001).
43. Ghattas, I.R., Sanes, J.R. & Majors, J.E. The encephalomyocarditis virus internal ribosome entry site allows efficient coexpression of two genes from a recombinant provirus in cultured cells and in embryos. *Mol. Cell Biol.* **11**, 5848–5859 (1991).
44. Pear, W.S., Nolan, G.P., Scott, M.L. & Baltimore, D. Production of high-titer helper-free retroviruses by transient transfection. *Proc. Natl. Acad. Sci. USA* **90**, 8392–8396 (1993).
45. Williams, B.P., Read, J. & Price, J. The generation of neurons and oligodendrocytes from a common precursor cell. *Neuron* **7**, 685–693 (1991).
46. Gowan, K. *et al.* Crossinhibitory activities of Ngn1 and Math1 allow specification of distinct dorsal interneurons. *Neuron* **31**, 219–232 (2001).
47. Mizuguchi, R. *et al.* Combinatorial roles of Olig2 and Neurogenin2 in the coordinated induction of pan-neuronal and subtype-specific properties of motoneurons. *Neuron* **31**, 757–771 (2001).
48. Lo, L., Tiveron, M.C. & Anderson, D.J. MASH1 activates expression of the paired homeodomain transcription factor Phox2a, and couples pan-neuronal and subtype-specific components of autonomic neuronal identity. *Development* **125**, 609–620 (1998).